Concrete shrinkage and creep under drying/wetting cycles

Yang Song, Qier Wu, Franck Agostini, Frédéric Skoczylas, Xavier Bourbon

Concrete shrinkage and creep under drying/wetting cycles

Yang Song[1, 2], Qier Wu[2], Franck Agostini[2], Frédéric Skoczylas*[1,2], Xavier Bourbon[3]

*corresponding Author: frederic.skoczylas@centralelille.fr

[1] Changzhou Institute of Technology, No.299 South Tongjiang Road, Changzhou China

[2] University of Lille, CNRS, Centrale Lille, LaMcube UMR9013, Lille, France.

[3] Andra, 1/7, rue Jean MonnetParc de la Croix-Blanche 92298 Châtenay-Malabry cedex

Note: Yang Song and Qier Wu have equally participated to this work. They have thus to be both considered as being the first authors of this paper.

Abstract:

Concrete shrinkage and creep under variable hydric conditions are important factors for the safety and durability of concrete especially in nuclear reactor or nuclear waste storage background. A large (and long – more than 900 days) experimental campaign, conducted on two different concretes, has therefore been designed to study the strains of non loaded and loaded concretes submitted to drying and liquid water imbibition cycles. For the purposes of comparison, concrete strains and mass variations during drying only (50% RH) and/or following cycles of drying/rewetting were also recorded. This allowed the identification of desiccation shrinkage, basic creep and drying creep at 10MPa of axial stress. Important results were found and have shown that the final mass and strain are not deeply modified by the introduction of a rewetting phase either for a loaded or a non loaded material.

Key words:

Shrinkage, Creep, cycle, drying, wetting

1 Introduction

ANDRA (Agence Nationale pour les Gestion des Déchets Radioactifs) in France is in charge of the radioactive waste storage management. High and moderate activity wastes would be likely stored at great depth (400-500m depth), into a clay rock (argillite) in concrete tunnels or in steel tubes for the more aggressive ones [1]. One of the main issues, encountered with this storage, is related to the "reversibility period", during which the wastes could be extracted from the storing structure to the surface for a period of 120 years. This means that, during this long time, a total integrity of the underground structures has to be preserved despite strong and various stresses: mechanical, chemical, hydraulic, thermal, etc. Among these, it can be mentioned that the concrete tunnels will be first partially dried due to inside temperature and ventilation. It will be then liquid water re-saturated through the interface with argillite, which is water saturated. As a result, ANDRA calculations and simulations of concrete tunnels have to take into account, among different properties, the concrete creep behaviour under drying, followed by imbibition with water. This is the main purpose of the present experimental study.

Among the properties of concrete, shrinkage and creep are key factors, as they can lead to large strains of a concrete containment structure, therefore influencing its level of safety. Concrete shrinkage and creep have been analysed in many research programs and studies [2-4]. These have mainly focused on the concrete's typical properties and environmental factors, such as: cement/water ratio, aggregates, relative humidity (RH) and temperature. Other factors being constant, a higher water/cement ratio leads to greater shrinkage and creep, whereas the adjunction of aggregates can reduce shrinkage and creep to a certain extent [3, 4]. Water saturation, which is affected by the ambient relative humidity, has a major influence on shrinkage and creep. The drying of concrete leads to greater strains, whereas rewetting induces swelling. In addition, Pickett [5] found that strains resulting from the drying of loaded concrete include the effects of autogenous shrinkage, drying shrinkage, basic creep and an additional

type of strain. The latter is now referred to as the Pickett effect or drying creep. Various mechanisms have been proposed to explain this effect and have been applied to predict drying strain effects. These include: micro-cracking theory, stress-induced shrinkage and microprestress-solidification theory [6-12]. Besides the deformation, water saturation also has great influence on concrete microstructure and mechanical properties. The drying of concrete may induce micro-cracks inside cement paste or between cement paste and aggregates. The rewetting could not only lead to self-sealing of microcracks, but also to changes in mechanical properties and to decrease in permeability and diffusivity.

A large part of the research on the strain of concrete has been made under constant humidity conditions, whereas very few studies [5, 13, 14] have been carried out using hydric cycle conditions. It has generally focused on modelling and/or strain occurrence mechanism of concrete under relative humidity (RH) changes. As concrete imbibition was caused by increases in RH rather than by direct contact with water[15], these studies can unlikely be applied to real in-situ saturation cases. Considerable differences are observed, even at 98% RH, since under these conditions the concrete is far from being fully saturated[16]. The latter occurs in the case of direct contact with water, and can induce notably different swelling strains. The strains experienced by non loaded and loaded concretes during hydric cycling remain therefore largely unknown and complementary experimental research is still needed, especially in the case of direct contact with water.

The aim of the research described in the present paper was to experimentally measure the shrinkage and creep experienced on two concrete candidates (called CEM I and CEM V), which are currently and deeply studied by Andra and its partners, during a drying (50% RH)/rewetting cycle. For the purposes of comparison, variations in concrete mass, shrinkage and creep were also monitored in three other states: initial state, continuous drying, and a single drying/rewetting cycle. Initial state means, in this research, that the mass sample (or its water

73 saturation) is supposed to remain constant during the whole testing process. It was generally
74 observed that this assumption is not completely true as some drying occurred despite the tight
75 envelope used to wrap the sample in "initial state".

76 **2 Experimental methodology**

77 2.1 Material and samples

78 Eight 16-32 cylinders of each concrete were provided by Andra. These were moulded using the
79 same kind of concrete (i.e. cement, w/c ratio, aggregate, superplasticiser) as that used by every
80 ANDRA partner laboratory. These concrete's formulations and properties have been described
81 in detail in various publications [17-22], which are not discussed here. The two concrete
82 compositions and some general properties are given in Table 1. Material porosities,
83 compressive strengths and Young's moduli were measured after six months of water cure on
84 cylindrical samples (37mm diameter and 70mm height). Porosity measurements were carried
85 out with classical vacuum technics with distilled water and sample dried at 105°C until stable
86 mass. Young moduli were obtained by unloading the samples from 10 to 1MPa. Strength and
87 Young's modulus were measured on water saturated samples.

88 **Table 1: About here**

89 The concrete cylinders were stored in lime-saturated water for approximately six months in the
90 laboratory. They were considered to be fully saturated at the end of this period. They were then
91 cored and cut to obtain 65 mm diameter, 65 mm high cylinders (Fig. 1). For the purposes of
92 rewetting, a 20 mm hole was drilled through the centre of each cylinder (Fig. 1). It is important
93 to note that the preparation of samples was done under great care and no cracks were observed.
94 They were then machined in order to get parallel surfaces within a tolerance of 0.01mm and to
95 minimize bending effects. The sample slenderness ratio was thus 1 and not 2 as it is usually

chosen. A compromise between the sample and device size (in order to use a unique climatic chamber) had to be found. The slenderness ratio might change the absolute results but (a priori) not the relative ones when the same sample is used in different scenario. Moreover numerous studies were performed on transfer properties (especially gas and relative gas permeability experiments) and they were not significantly affected by this reduced slenderness ratio.

Figure 1: about here

A total of 42 samples were randomly chosen and prepared for three different curing conditions (Table 2): initial (endogeneous) state (i.e. external surface completely sealed), drying (50% RH and 25°C), drying/rewetting (50% RH, pure water into the 20mm hole and 25°C). The following measurements were made under each of these conditions: mass variation, strain of the non-loaded samples, strain of the loaded samples. As it is uneasy to weigh samples equipped with wires and LVDT sensors, it was chosen to record mass variation on seven (for each concrete) witness samples. These (non-instrumented) samples were prepared and preserved in the same conditions as the instrumented ones.

Table 2: About here

2.2 Test devices

Sample under endogenous conditions

Six concrete samples were first wrapped in aluminium foil then coated with a watertight glue to prevent the exchange of water moisture (Fig. 2). These could thus be expected to remain in their initial state, i.e. to have no exchange of water. They were placed in an air-conditioned room, in which the temperature was set to remain at 25°C, for more than 500 days.

Figure 2: About here

Samples submitted to drying and wetting-drying phases

The remaining tests (drying, rewetting and drying) were carried out in a 240L climatic chamber, at 50% RH and 25°C, for more than 900 days. These were considered to be close to the average values experienced under standard environmental conditions.

In addition, imbibition (during the rewetting/drying operations) was achieved by filling the central hole of each concrete sample with water. Both ends of the samples were bonded to a steel plate with a special waterproof copolymer mastic PU/silicone-MSP15 type (in red in Fig. 3a and 3b), thus allowing them to be filled with water. This mastic can stand strains as high as 200% and its Young's modulus is less than 1MPa. Its mechanical (lateral) effects on concrete sample can therefore be assumed to be negligible.

Interior ducts were connected to a water reservoir using two plastic tubes (Fig. 3), allowing the samples to remain filled with water siphoned from a reservoir. Note that distilled water was used to avoid minerals added during the rewetting. This device allowed water to be continuously supplemented to make up for water imbibition and evaporation. LVDT sensors were used to evaluate sample axial strains (Fig.3a).

The samples intended for mass variation measurements were prepared in the same way to ensure the same boundary conditions, especially the hydric ones. For obvious reasons, they were not equipped with LVDT sensors. The mass variations were determined by weighing these samples on scales with an accuracy of 0.01 g. Except for the wetting phases, it will be assumed in the result analyses that the relative humidity level inside the 20mm sample hole is the same as in its surrounding (RH 50%). The relative humidity equilibrium between the hole and the

surrounding air occurs through the two input water and drainage tubes. This is controlled by water vapour diffusion into air at 25°C. At this temperature the water vapour permeability in air is around 0.7 mg.(m.h.Pa)$^{-1}$. The water vapour mass in sample 20mm hole is 0.4mg at RH100% and 0.2mg at RH50%. A rapid calculation showed that the required time to get RH50% from RH100% in the hole (i.e. to lose 0.2mg of water vapour) is less than one hour. It is therefore logical to assume that the humidity in the tube remains at RH50%.

Figure 3: About here

Figure 4: About here

The sample axial strains were measured with linear variable differential transducers (LVDT) having a 2mm stroke [-1mm, +1mm]. Prior to installing the LVDT, two aluminium rings separated by 30 mm were attached to the samples with six screws (Figs. 3a and 4). The LVDT was then attached to the upper ring with its tips remaining in contact with the lower ring, thus allowing the concrete's longitudinal strains to be measured. Note that only two LVDT were used to record the strains. It is commonly admitted that it is preferable to use three LVDT to get the mean axial strain but, in the present case, it was not possible for space and cost reasons.

A steel frame was designed to load the samples with a compressive uniaxial stress of 10 ± 0.33 MPa. The load was applied through a spherical contact thus also limiting possible bending effects (Fig.3b and Fig.4a). This device was made from four coupling bolts (equipped with belleville washers), two steel plates and one stress transducer. When installed between the upper plate and the sample, it allows a sample's stress to be continuously recorded. The force can be adjusted as required, by tightening or loosening the bolts. Such adjustments were made

165 regularly, especially at the beginning of the drying and rewetting phases: shrinkage or creep led
166 to stress relaxation, whereas swelling led to a considerable increase in stress. As indicated in
167 Fig.5, the difference between LVDT signals was generally less than 8-10%. It can also be
168 mentioned that if some bending occurred, the bending axis would likely be a tube section
169 diameter (rotation axis in pure bending). Averaging signals from diametrically opposed LVDT
170 is thus supposed to compensate these parasitic effects i.e. giving the mean axial sample strain.
171 On the other hand this disposal and these strain measurements do not allow to highlight local
172 effects such as drying or shrinkage heterogeneity and do not give any information on radial
173 strains.

174 All of the stress and strain values were automatically recorded using an in-house routine
175 developed under the Labview system (Fig.4b). The LVDT and stress transducers were carefully
176 calibrated before the experiment.

177

178 **Figure 5: About here**

179 2.3 Experimental procedure

180 Following preparation of the devices and calibration procedures, all of the tests were initiated
181 at the same time, the concrete's age was thereby identical for every tested sample. Strains of the
182 concrete samples were recorded automatically, once every 15 minutes. The sample's mass was
183 recorded manually every 24 hours during the first 7 days of each drying or rewetting phase, and
184 thereafter every 7 days. It should be noted that the influence of instantaneous strains on the
185 loaded samples is neglected, since the aim of the experiment was to focus on creep and
186 shrinkage (or swelling) only.

During the so-called "drying/rewetting phases", the concrete samples were firstly dried for 260 days or 460 days, then rewetted with pure water, and finally dried again from 654 days to the end of the experiment. A generic numbering of samples can be found in table 3 that sums up the different hydric conditions and duration. This generic numbering (excluding endogenous state) is valid for each concrete and for any kind of measurement (mass or strain). In the following figures (S.n-m-p) in a legend means that the result is the average value obtained on samples n° n, m and p.

Table 3: About here

3 Results and discussion

3.1 Mass variation

Fig. 6 plots the average mass variation recorded for the two sets of concrete samples submitted to drying only. As it is mentioned in Table 2, the average value is obtained with three samples CEMI or CEMV. These results show that the drying kinetics of the CEMV is slower than that of the CEMI. This phenomenon had been found in many previous studies as the CEMV concrete is an evolving concrete with an initial porosity finer than that of the CEMI. The CEMV cement is constituted of 60% clinker in mass, 22% blast-furnace slag, 14% fly ash and 4% setting regulator (NF EN 196-4 European Standard). Due to delayed hydration of the CEMV cement, the CEMV concrete porosity is getting finer and finer with time [17]. For the latter, the equilibrium state seems to be achieved in around 900 days of drying. There are two phases for the CEMI concrete. The stable mass seems to be reached in 250 days until 400 days (this is the first phase). Following this period of time, there is a second phase, which shows a slight and progressive increase in mass. The main hypothesis is that there is a material carbonation, which is plausible at 50%RH for this concrete composed with CEMI cement. In fact CEMI concrete is well known to contain a large amount of calcium hydroxide ($Ca(OH)_2$) able to form calcium

211 carbonate ($CaCO_3$) with CO_2. In addition the use of a closed hermetic chamber is known to
212 intensify the ambient CO_2 concentration, thereby accelerating carbonation of concrete [3, 4]. The
213 present results do not allow to quantify the mass variation due to carbonation. It is also well
214 known that carbonation is likely to induce additional shrinkage i.e. carbonation shrinkage,
215 which is also unknown.

216

217 **Figure 6 : About here**

218 In Fig. 7a can be found the average results (obtained on two samples of each concrete) recorded
219 for a first phase of 260 days of drying then followed with water imbibition for 400 days. It can
220 be firstly underlined that this imbibition has instantaneous effects on the two concrete
221 saturation. The new mass equilibrium state is reached in a few days for the CEMI whereas two
222 months are needed for the CEMV. A second remarkable aspect lies in the mass amplitude
223 regained by both concretes, 77% for the CEMI and 37% for the CEMV. This means that, for
224 this kind of experimental conditions (liquid water inside the tube and 50%RH around the
225 sample), the loss in mass in not reversible. The equilibrium is therefore the result of imbibition
226 from the borehole and drying at the external surface. Imbibition is extremely rapid for the
227 CEMI. The case is different for the CEMV as its imbibition is slower than for the CEMI. As a
228 consequence, it can be supposed that the CEMV mass equilibrium is more affected by the
229 external drying and finally leads to a lower gain in mass. It can also be assumed that the evolving
230 porosity of the latter can play a significant role on the gain in mass difference. Fig. 7(b) plots
231 the results obtained after the second drying phase. A similar behaviour is found compared with
232 the first drying. Taken into account that different samples were used for the only drying
233 experiments and for the drying/imbibition/drying ones, it can be considered that the CEMI
234 concrete mass has returned on the same red curve (only drying). This means that the

imbibition/drying operation is likely to be reversible (on a water mass content point of view). The CEMV concrete had not reached its equilibrium yet but the tendency would indicate the same phenomenon. It can be seen, in Fig. 4, that the points A, B are very close (for CEMI) but C and D (for CEMV) are still distant. On another hand the slope V clearly indicates that the hydric equilibrium is far to be reached. It cannot be concluded that the mass content variation due to drying/imbibition/drying phase (compared with drying only) is reversible but it is likely to be for the CEMI and plausible for the CEMV after a longer drying time.

Figure 7: About here

One sample of each material was submitted to the same drying/imbibition/drying operation but delayed by 200 days (Fig. 8). The gain in mass for the CEMI is virtually the same, which is logical as the samples used (imbibition at 260 or 460 days) had almost reached the same mass equilibrium state i.e. the same level of capillary suction. The situation is different for the CEMV as now the mass equilibrium state stabilizes faster and at a higher mass level (point E compared with F in Fig. 8). The initial state of drying -before imbibition- is very different for the CEMV at 260 or 460 days. This means that at 460 days the capillary suction is higher than at 260 days whereas the water saturation is lower. This can explain the gain-in-mass difference (37% at 260 days and 53% at 460 days) and the change in (re) saturation kinetics. Both concretes do not meet their initial mass after imbibition. This can be due to the experimental procedure, which does not lead to homogeneous conditions i.e. liquid water in the borehole and 50% RH at the external sample surface. This means that the gain in mass is resulting from a balance between imbibition (gain) and surface drying (loss). It is also possible that some air bubbles remain

entrapped in the materials. One can add that different concrete properties are involved in such a balance: water vapour diffusivity, water and relative water permeability, pore distribution and also possible micro-cracking. If they are different then the final mass equilibrium will not be the same (point E compared to point F). For a purpose of control, two witness samples (one CEMI and one CEMV) were water vacuum re-saturated after 900 days of drying and their mass was slightly higher than at the beginning of the first drying: +0.09% for the CEMI and +0,04% for the CEMV. These small differences are not very significant and evidence, that after a long drying, these materials can almost meet their initial water content. On the other hand it is remarkable that the following drying, performed at the same time (654 days), leads to similar drying curves and virtually identical final state (at 900 days) for samples of each concrete.

Figure 8: About here

Even if this aspect is further on analysed, it is interesting to observe in Fig. 9 that the drying shrinkage v.s. mass loss is higher for the CEMV than for the CEMI (fact frequently attributed to its finer porosity). For both materials the global shrinkage, at the end of the second drying operation, is slightly higher than after the first one (see the circles on Fig. 9). As the difference between both is less than 8% it could be assumed, on a first order, that the final shrinkage is not deeply influenced by the intermediate imbibition/drying phase, which nevertheless leads to higher shrinkage strains for the second drying. This is a general trend as potential carbonation may also induce a bias on both mass variation and strain. Hence the relationship between shrinkage and mass variation is unlikely to be purely hydro-mechanical.

Figure 9: About here

283 Figure 10 plots the mass variation of samples protected from desiccation. Despite every
284 precaution taken to avoid the latter, it can be seen that a very small loss in mass occurred for
285 both concrete (around 0.15%) after 900 days of experiment. However, this phenomenon had
286 not a significant influence on the autogenous shrinkage ε_{as} as it is detailed in the following. It
287 can also be underlined that the samples were protected from desiccation with two layers of a
288 special epoxy resin, which contains some solvent. The solvent evaporation can also induce a
289 part of the mass loss measured for this test.

290

291 **Figure 10: About here**

292 3.2 Strains under endogenous conditions – basic creep

293 There is an usual decomposition for strains due to creep and desiccation. In its initial state (i.e.
294 protected from desiccation), the strain of a free loaded sample results mainly from autogenous
295 shrinkage ε_{as}, whereas in the case of loaded concrete, the strain ε_i is considered to include both
296 autogenous shrinkage and basic creep ε_{bc} [23, 24].

297 $$\varepsilon_i = \varepsilon_{as} + \varepsilon_{bc} \quad (1)$$

298 In the case of drying only, the strains of a non loaded concrete ε_{df} include both autogenous
299 shrinkage and drying shrinkage ε_{ds} [23, 24].

300 $$\varepsilon_{df} = \varepsilon_{as} + \varepsilon_{ds} \quad (2)$$

301 Conversely, the strains of a loaded concrete sample ε_{dl} can be considered to result from the
302 combined effects of four different components.

303 $$\varepsilon_{dl} = \varepsilon_{as} + \varepsilon_{bc} + \varepsilon_{ds} + \varepsilon_{dc} \quad (3)$$

304 ε_{dc} is the drying creep of concrete (known as Picket effect), which considerably amplifies the
305 final strain.

306 In Figure 11 can be found the strains (ε_{as}) for samples preserved under protected conditions. As
307 mentioned before, they had been previously stored in water for more than 6 months. It was thus
308 logical to record virtually negligible strains after such a period of time, which is generally
309 sufficient to consider that autogenous shrinkage is no longer present. It can also be underlined
310 that there is no strain associated to the loss in mass of 0.15% of the witness samples.

311

312 **Figure 11: About here**

313 As a result, the strains measured for the protected loaded sample will be directly related to the
314 basic creep ε_{bc}. They are given in Fig. 12 in which it can be seen that the basic creep (at 10MPa
315 axial stress) stabilized after around 200 days for the CEMV and 450 days for the CEMI. The
316 basic creep final amplitude is higher for the CEMI than for the CEMV (≈160μm/m compared
317 with ≈130μm/m). These values were recorded for 600 days as some tightness issues occurred
318 after this duration of testing. To extrapolate until 900 days of tests, exponential fits were used
319 to evaluate the drying creep, which is presented in the following.

320 For the CEMI: $\varepsilon_{bc} \approx -160(1 - e^{-\alpha t})$ with α=0.009

321 For the CEMV: $\varepsilon_{bc} \approx -130(1 - e^{-\beta t})$ with β=0.035

322 These values are calculated in μm/m and t is the time in days. As mentioned before the
323 asymptotic levels of ε_{bc} are 160 and 130μm/m.

324

325 **Figure 12: About here**

A comparison between the results obtained in this study and what can be found in the literature is given in Fig. 13. These previous results were extracted from Ladaoui PhD thesis [17] and summed up basic creep for the two water cured concretes (i.e. without the elastic strains). All these results can be considered to lie in the frame of visco-elasticity as the applied stresses were less than 30% of the material strength. It has to be noted that the creep tests were conducted at 12-14 months for Camps [25] and Ladaoui and more than 5 years for CEBTP [26]. This time difference may explain the lower creep amplitude obtained in the CEBTP measurements. The present results are similar to those of Camps and Ladaoui for the CEMI concrete even if the initial kinetic is lower. The CEMV concrete exhibits a higher amplitude but the global aspect is similar. Given the fact that between the different studies the cements used are not exactly identical (i.e. not provided by the same factory and at different years) as well as the testing conditions (size, age of samples, stress rate), it can be considered that the present results are consistent with several former ones.

Figure 13: About here

One mechanism for basic creep comes from microprestress-solidification theory [8, 27, 28]. It considers that the basic creep is determined by activation energy barrier for bond breakage of hydrated cement paste. Once the activation energy barrier for bond breakage has been reached, the bonds and bridges between slipping planes break down, and microstructural creep occurs.

3.3 Strains under drying conditions – drying creep

In Figures 14 and 15 are respectively plotted the basic creep ε_{bc}, the desiccation shrinkage ε_{ds} and the total creep ε_{dl} for the CEMI and CEMV concretes. From relation (3), as ε_{as} is negligible, the drying creep can be extracted with $\varepsilon_{bc}=\varepsilon_{dl}-\varepsilon_{bc}-\varepsilon_{ds}$. This operation leads to the results plotted in Fig. 16.

Figure 14 : About here

Figure 15 : About here

Figure 16: About here

There are two distinct parts in the drying creep evolution: a rapid increase of large amplitude strain (50% of the final drying creep) for the CEMI whereas it is smoother for the CEMV. These results can be observed in parallel with Fig. 6 related to the loss of mass under drying, which is significantly faster for the CEMI. Obviously, this faster mass variation is linked to the kinetics of the drying shrinkage evolution at the beginning of loading. Following this first part, both concrete drying creep are quasi linear with similar slopes. After 900 days of measurements, the drying creep is respectively 35% and 25% of the total creep for CEMI and CEMV concretes. It can be also noted that, even if the drying shrinkage is virtually stabilized for both concretes (Figs. 14 and 15), the drying creep is still evolving. Additional results, which include sample 6, do not seem to change the general tendency previously described.

3.4 Strains under drying/imbibition operations

This last part is related to the case for which both concretes were submitted to liquid water imbibition after a first phase of drying. This kind of testing was performed in two phases for each concrete: imbibition of four samples (2 loaded and 2 non-loaded) after 260 days of drying and imbibition of two remaining samples (1 loaded and 1 non-loaded) after 460 days of drying. The six samples were then dried again at 654 days until the end of the experiment (900 days).

3.4.1 CEMI results

The results obtained for the first imbibition (at 260 days) are given in Figure 17 for the CEMI. As it was observed for the mass variation, the imbibition effects on strains are quasi-instantaneous. After 6 days of imbibition, which is very short, the average strain variation for

376 the non loaded samples is +180µm/m and +200µm/m for the loaded ones. This behaviour is in
377 agreement with previous results [3], which have shown that the shrinkage reversibility of normal
378 strength concrete (compressive strength from 10 to 40 MPa) ranges between 40% and 70%
379 during the first rewetting phase. The strains for non loaded samples stabilized quite fast, which
380 is logical as its water content is constant (see Figs. 7 and 8). There is no particular loading effect
381 in this case and the compressive stress does not play a limiting role on the swelling. It is also
382 interesting to mention that after imbibition the creep has almost stopped whereas the total creep
383 (under drying) is still evolving. At 654 days the samples are submitted to drying again, which
384 led to a new phase of shrinkage. The non loaded sample strains did not completely match the
385 initial tendency (extrapolation from D to C and point B compared with point C) but the
386 difference, which is quite small, could still decrease after a longer time than 900 days. This is
387 in agreement with several previous results [3, 29]. The loaded sample strains clearly meet the
388 initial tendency (extrapolation from F to A and point E compared with point A).

389 The delayed imbibition had been performed on two samples only (1 loaded and 1 non loaded).
390 The main goal of this operation was to confirm (or not) what had been observed for the first
391 imbibition phase. The sample behaviour can be analysed (and compared with the previous one)
392 in Figure 18. There is an “immediate” swelling following imbibition with amplitudes of
393 +160µm/m for the non-loaded sample and +150µm/m for the loaded one. The difference
394 between both does not seem significant i.e. no particular effect due to loading on the swelling.
395 On a global point of view the behaviour observed in this second imbibition phase is similar to
396 the previous one. One can nevertheless mention that the non-loaded sample swelling slightly
397 increases with time but, when the samples are dried again, the strain curves meet up with the
398 initial tendency for both cases (non-loaded and loaded).

399

Figure 17: About here

Figure 18: About here

3.4.2 CEMV results

The results for the first imbibition (at 260 days) are given in Fig. 19 for the CEMV. There is still a rapid swelling, which is very contrasted according the sample status: +90μm/m for the non loaded samples and +160μm/m for the loaded ones. This spectacular difference will not be observed for the delayed imbibition case (and was not for the CEMI). It cannot be concluded that there would be an 'inverse' Picket effect. As its water content is constant (see Figs. 7 and 8), the non loaded material strains remained almost constant during this imbibition phase. The drying was performed at 654 days that led logically to shrinkage and a new drying curve that meets the initial tendency (see point C compared with point B obtained from an extrapolation of A). The main difference between the CEMV and the CEMI concrete lies in the loaded sample behaviour. After the initial swelling, the loaded CEMV samples still exhibit a significant creep (not the case for the CEMI sample); there is then a strain stabilization from around 400 to 654 days. This phase of creep during the beginning of the first imbibition is questioning. Its duration is more or less the necessary time for the sample mass to be stable (see Fig.8) and this stabilization results from the balance between drying at the surface and imbibition inside the hole. This new creep can unlikely be attributed to basic creep reactivation as the previous results had shown that its stabilisation occurred around 200 days (see Fig. 12). At this stage this new creep phase is difficult to explain without complementary investigations, especially because structural effects are involved.

When dried again at 654 days the induced material shrinkage does not completely meet up with the initial tendency. However, the difference (at 900 days) is weak and the comparison between slope 1 and slope 2 makes possible to assume that the gap between point F and E would continue to reduce with time.

The delayed imbibition (at 460 days) led to results that are plotted and compared with the previous ones in Fig. 20. The initial swelling amplitude is now: +158µm/m for the non loaded sample and +175µm/m for the loaded one. Even if slightly higher for the loaded sample, the difference between both swellings is not very significant. This result, which is consistent with the CEMI case, is likely to indicate that the swelling differences measured for the first CEMV imbibition are artefact or particular case. It can be underlined that the non loaded sample does not exhibit any shrinkage during its imbibition phase. The following drying does not lead to points I and H (initial tendency extrapolation) merging but the hydric equilibrium is not reached yet. As for the previous case it can be assumed that the merging would occur after more than 900 days. The behaviour of the loaded sample is very similar to the one observed for the first imbibition, especially between 470-654 days, which is the common time interval for both families of sample. There is no creep to be observed in this second case, which is quite logical as the basic creep is stabilized. After drying, this sample is close to meet its initial tendency (point L and K – Fig.20).

As a whole, it can be observed that, even if performed at different time during the drying (and/or drying and loaded), the intermediate phase of imbibition/drying does not deeply modify the initial shrinkage tendency (for both concretes) and eventually leads to a “statu quo”. To summarise these effects, the drying/rewetting/drying cycle does not induce significant additional strains, and rewetting may slightly reduce the final strain. This result is quite meaningful for the safety of concrete containment, since this material is more likely to experience drying/rewetting cycles than constant drying or wetting.

448

449

450 **Figure 19: About here**

451

452

453 **Figure 20 : About here**

454

455

456 **4. Conclusion**

457 The main objective of this (necessary long – 900 days) experimental study was to evaluate the
458 effects of intermediate wetting-drying operations during a drying phase of two different
459 concretes CEMI and CEMV, they were either non-loaded or loaded (10MPa constant axial
460 stress). The wetting phase was performed with liquid water to match some encountered in-situ
461 cases. A special interest was to bring into focus the strains and, to a lesser extent, the mass
462 variation of samples submitted to these different hydric changes. Several important and
463 interesting results can be drawn from this study.

464 *About mass variation*

465 Two intermediate wettings with liquid water were carried out at 260 (1) and at 460 days (2),
466 both were maintained until 654 days. The samples were then dried again. Both concretes did
467 not meet their full initial water saturation but this is mainly due to the imbibition system that
468 was carried out with liquid water inside the sample hole. The resulting sample water saturation
469 was therefore a combination of water absorption and surface evaporation. Under wetting, the

relative gain in mass was higher at 460 days than at 260 days for the CEMV. It is, on a first order, a direct consequence of the lower saturation at 460 days than at 260 days. The situation is different for the CEMI as its mass was already stable after 260 days. As a consequence, its gains in mass were found to be similar for both wettings despite the bias due to potential carbonation. The second drying, performed at 654 days, showed that both families of concrete have their own behaviour but exhibit similar (new) drying curves as the first ones. Even if plausible, it can not be assessed that the materials will finally meet their initial drying curves but the gap will be small.

About strains vs time for loaded or free loaded samples

The global results show similar tendencies for both concretes as regards the strain evolutions under drying or drying-wetting-drying phases. As for the mass variation, the rewetting process led to an immediate swelling, which is not highly influenced by the loading. There is no "inverse" Picket effect. The following drying (drying phase after imbibition) led to a new shrinkage that almost brings back the drying curve to the extrapolated initial one. This was systematically observed for the two materials. Imbibition of loaded sample also led to immediate swelling that was followed by a plateau (i.e. almost no strain evolution) until the second drying. When dried again, there is a new shrinkage that almost brought back all the loaded samples to their initial shrinkage curve. As a whole, it can be concluded that the intermediate wetting (with liquid water) – drying cycle leads to very small difference in strains, compared with drying only. This was observed for loaded or non-loaded samples.

That means that for in-situ cases, imbibition, thanks to the swelling produced, will lead to crack closure and a partial recovery of the structure tightness. On the other hand, if this phase is followed with a new drying, there will likely to be no additional shrinkage strain.

494 Disclosure statement: No potential conflict of interests was reported by the authors

495 Fundings: The authors wish to thank Andra for its financial support and for the concrete core
496 supplying

497

Reference

[1] YANG S, DAVY C A, TROADEC D. Gas Breakthrough Pressure (GBP) through Claystones: Correlation with FIB/SEM Imaging of the Pore Volume [J]. Oil & Gas Science & Technology, 2016, 71(4): 51.
[2] BROOKS J J. Creep of Concrete [J]. 2015, 281-348.
[3] BROOKS J J. 6 - Shrinkage of Concrete [M]//BROOKS J J. Concrete and Masonry Movements. Butterworth-Heinemann. 2015: 137-85.
[4] NEVILLE A M. Properties of concrete [M]. 1995.

[5] PICKETT G. Shrinkage stresses in concrete; proceedings of the ACI Journal Proceedings, F, 1946 [C]. ACI.
[6] BAZANT Z, WU S. Rate-type creep law of aging concrete based on Maxwell chain [J]. Materiaux et Construction, 1974, 7(1): 45-60.
[7] BAZANT Z, YUNPING X I. Drying creep of concrete: constitutive model and new experiments separating its mechanisms [J]. Materials and Structures, 1994, 27(1): 3-14.
[8] BAZANT Z P, CUSATIS G, CEDOLIN L. Temperature effect on concrete creep modeled by microprestress-solidification theory [J]. Journal of engineering mechanics, 2004, 130(6): 691-9.
[9] BAZANT Z P, WANG T-S. Practical prediction of cyclic humidity effect in creep and shrinkage of concrete [J]. Materials and Structures, 1985, 18(4): 247-52.
[10] BAZANT Z P, WU S T. Thermoviscoelasticity of aging concrete [J]. Journal of the Engineering Mechanics Division, 1974, 100(3): 575-97.
[11] ROSSI P, TAILHAN J-L, LE MAOU F. Comparison of concrete creep in tension and in compression: Influence of concrete age at loading and drying conditions [J]. Cement and Concrete Research, 2013, 51(78-84).
[12] WITTMANN F, ROELFSTRA P. Total deformation of loaded drying concrete [J]. Cement and Concrete Research, 1980, 10(5): 601-10.
[13] VANDEWALLE L. Concrete creep and shrinkage at cyclic ambient conditions [J]. Cement and Concrete Composites, 2000, 22(3): 201-8.
[14] BAZANT Z, CHERN J. Concrete creep at variable humidity: constitutive law and mechanism [J]. Materials and structures, 1985, 18(1): 1-20.
[15] CAGNON H, VIDAL T, SELLIER A, et al. Drying creep in cyclic humidity conditions [J]. Cement and Concrete Research, 2015, 76(91-7.
[16] CHEN W. Etude expérimentale de la perméabilité du béton sous conditions thermiques et hydriques variables, PhD thesis; Ecole Centrale de Lille, Université de Lille1, France2011.
[**17**] LADAOUI W, Etude expérimentale du comportement Thermo_Hydro-Mécanique à long terme des BHP destinés aux ouvrages de stockage des déchets radioactifs, PhD thesis, Université de Toulouse, France, 2010

[**18**] RANAIVOMANANA H, VERDIER J, SELLIER A, BOURBON X, Toward a better comprehension and modelling of hysteresis cycles in the water sorption-desorption process for cement based materials, Cem. Concr. Res. 41 (2011) 817-827

[**19**] BRUE F, DAVY C.A, SKOCZYLAS F, BURLION N, BOURBON X, Effect of temperature on the water retention properties of two high performance concretes, Cem. Concr. Res. 42 (2011) 384-396

[**20**] BRUE F, DAVY C.A, BURLION N, SKOCZYLAS F, BOURBON X, Five year drying of high performance concretes: Effect of temperature and cement-type on shrinkage, Cem. Concr. Res., 99 (2017) 70-85

[**21**] ZHANG Y, Comportement hydrique et poro-mécanique des bétons à hautes performances Andra, PhD thesis LML, Université de Lille 1, France, 2014

[**22**] CHEN W, LIU J, BRUE F, SKOCZYLAS F, DAVY C. A, BOURBON X, TALENDIER J, Water etention and gas relative permeability of two industrial concretes, Cem. Concr. Res., 42 (2012) 1001-1013

[23] GAMBLE B, PARROTT L. Creep of concrete in compression during drying and wetting [J]. Magazine of concrete research, 1978, 30(104): 129-38.

[24] DAY R, CUFFARO P, ILLSTON J. The effect of rate of drying on the drying creep of hardened cement paste [J]. Cement and Concrete Research, 1984, 14(3): 329-38.

[**25**] CAMPS G, Etude des interactions chemo-mécaniques pour la simulation du cycle de vied'un élément de stockage en béton, PhD thesis, Université de Toulouse, France, 2008

[**26**] CEBTP, Etude de l'action chimique et mécanique couplée sur les propriétés des bétons CEM I et CEM V après une longue cure, LMDC/Andra: Contrat CR 8C 442, Rapport N° D BPD 1 9 017, Etat d'avancement N°2, France, 2010

[27] BAZANT Z P, HAUGGAARD A B, BAWEJA S, et al. Microprestress-solidification theory for concrete creep. I: Aging and drying effects [J]. Journal of Engineering Mechanics, 1997, 123(11): 1188-94.

[28] BAZANT Z P, HAUGGAARD A B, BAWEJA S. Microprestress-solidification theory for concrete creep. II: Algorithm and verification [J]. Journal of Engineering Mechanics, 1997, 123(11): 1195-201.

[29] NEVILLE A M, BROOKS J J. Concrete technology [M]. Longman Scientific & Technical Harlow, 1987.

List of figures

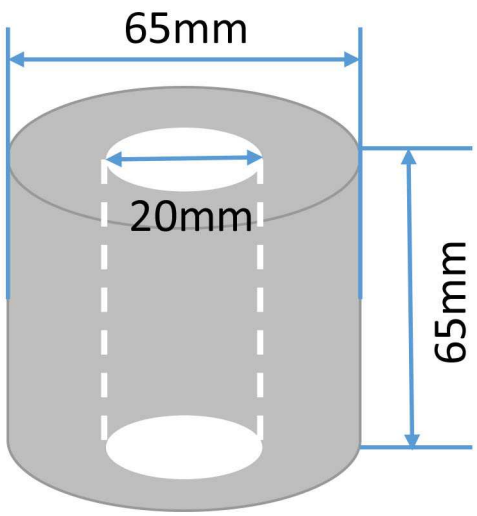

Figure 1: Preparation of concrete sample

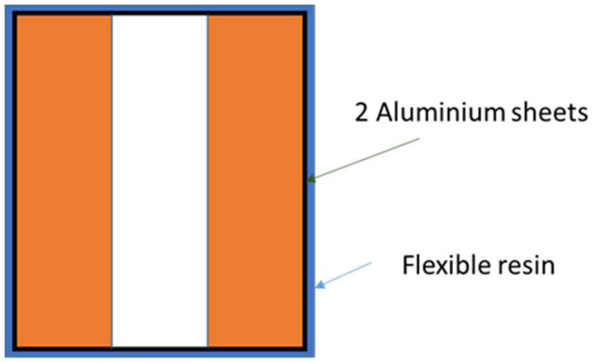

Figure 2: Preparation of sample under endogenous conditions

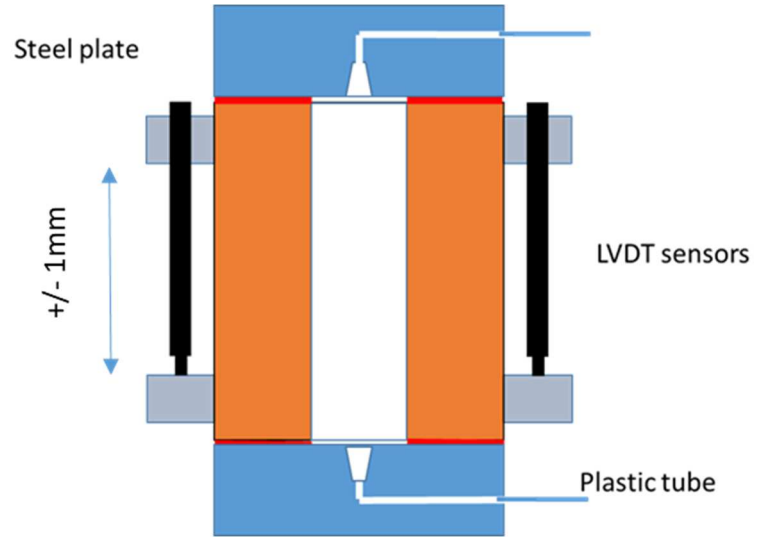

(a)

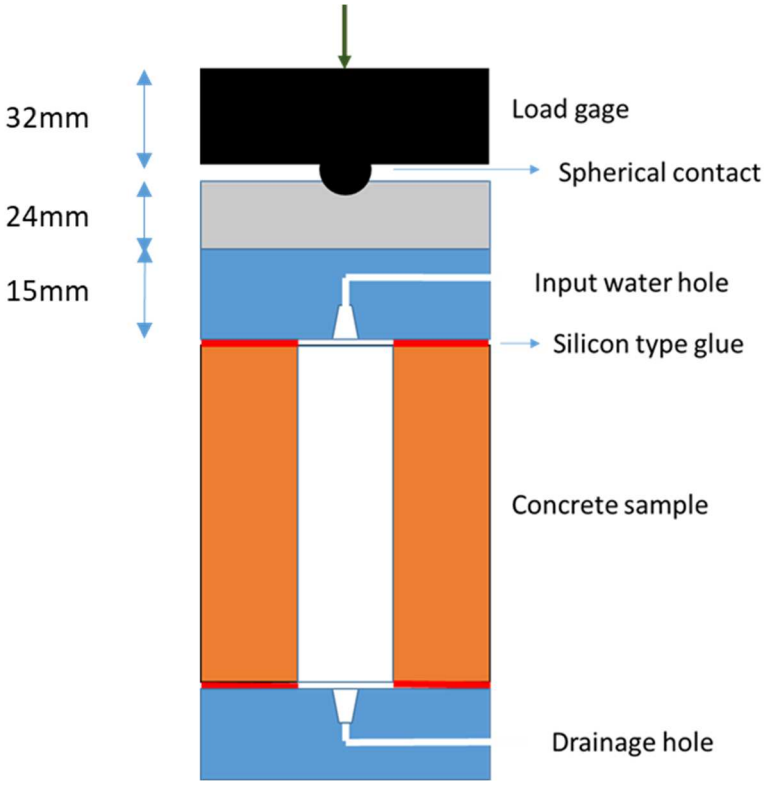

(b)

Figure 3: Preparation of concrete cylinders: (a) equipped with LVDT sensors and (b) with loading disposal

(a)

(b)

Figure 4: Concrete samples prepared for the test: (a) loaded samples, (b) acquisition system (Labview) used to record the stress and strain evolution.

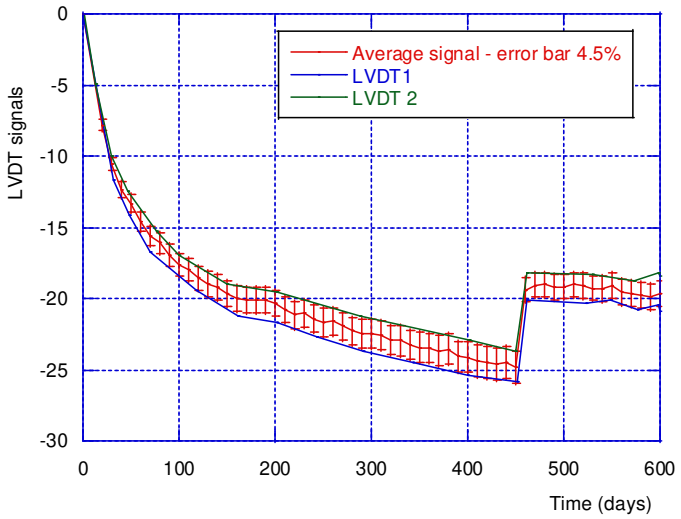

Figure 5: Example of recorded LVDT signals

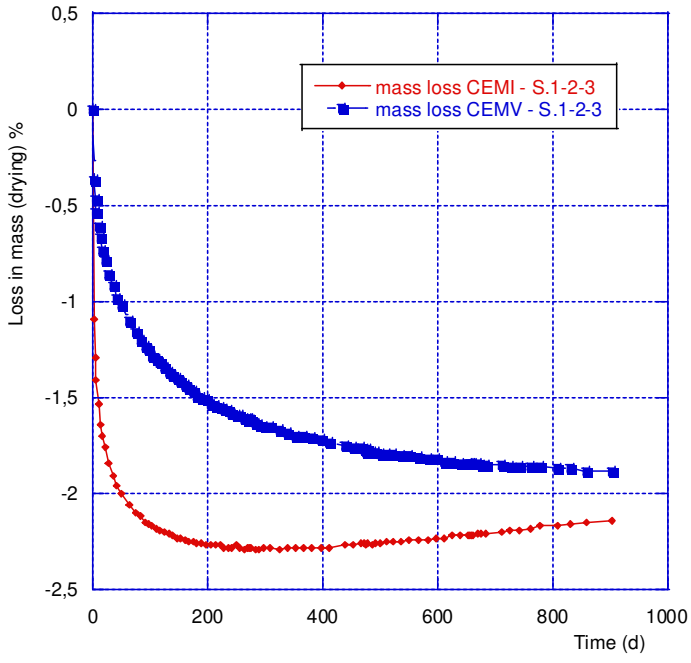

Figure 6 : Relative mass variation for both concretes-Drying at 50%RH – Samples 1-2-3

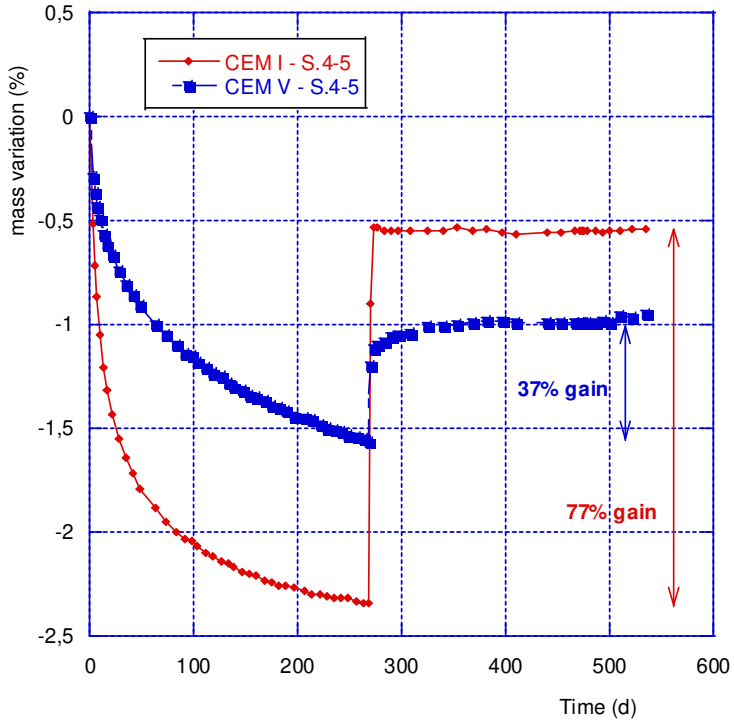

(a)

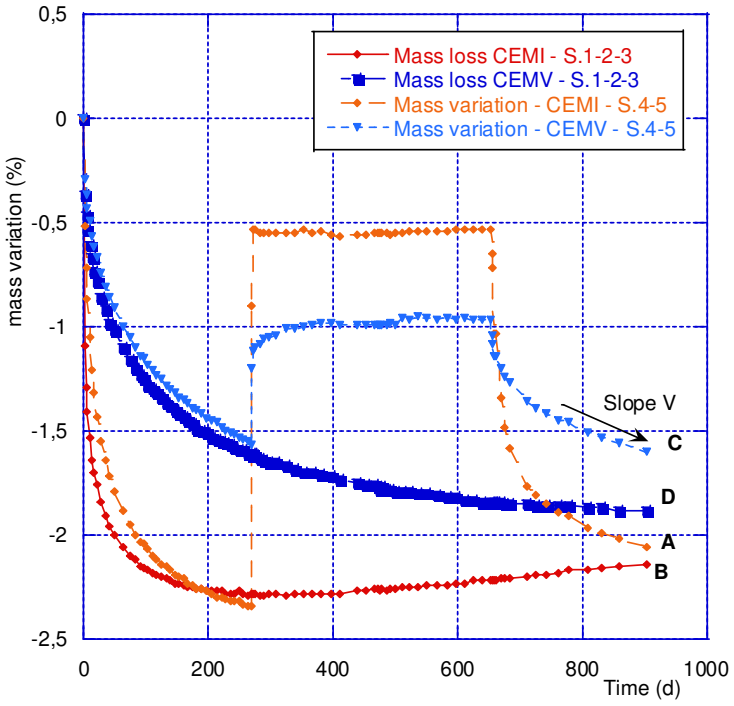

(b)

Figure 7: Mean relative mass variation for both concretes - drying followed by imbibition (a) – after the second drying (b)

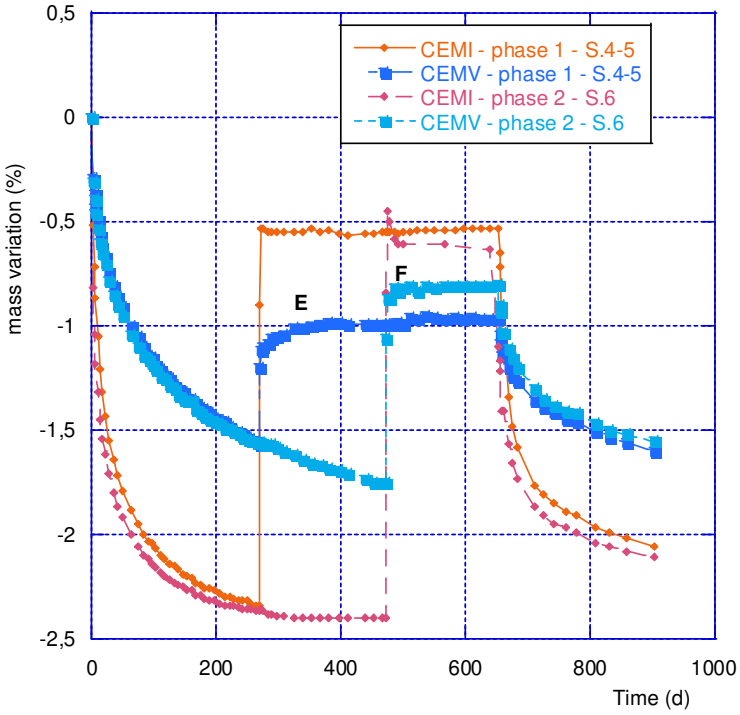

Figure 8: Mean mass variation for both concretes under drying – wetting and second drying

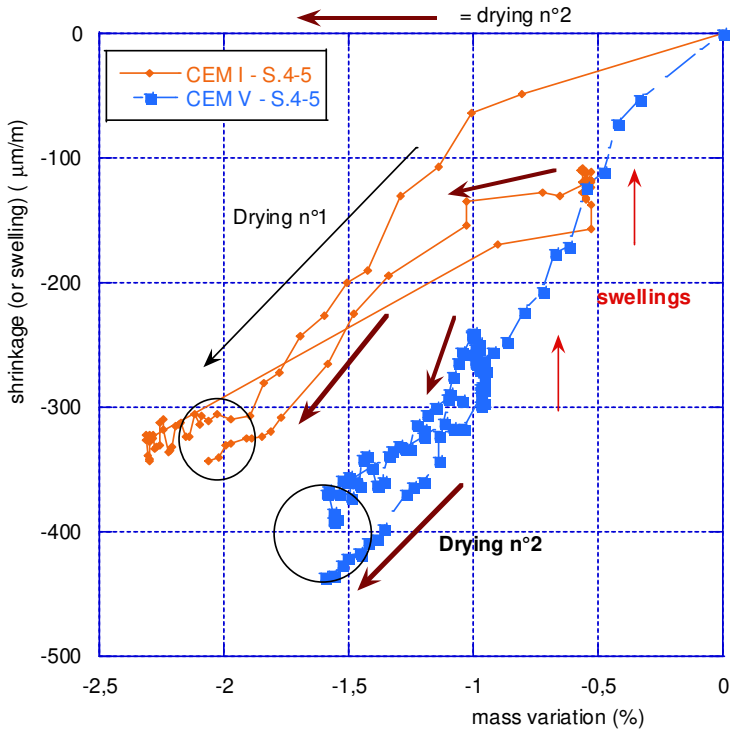

Figure 9: Strains due to drying – imbibition – second drying (indicated with bold arrows)

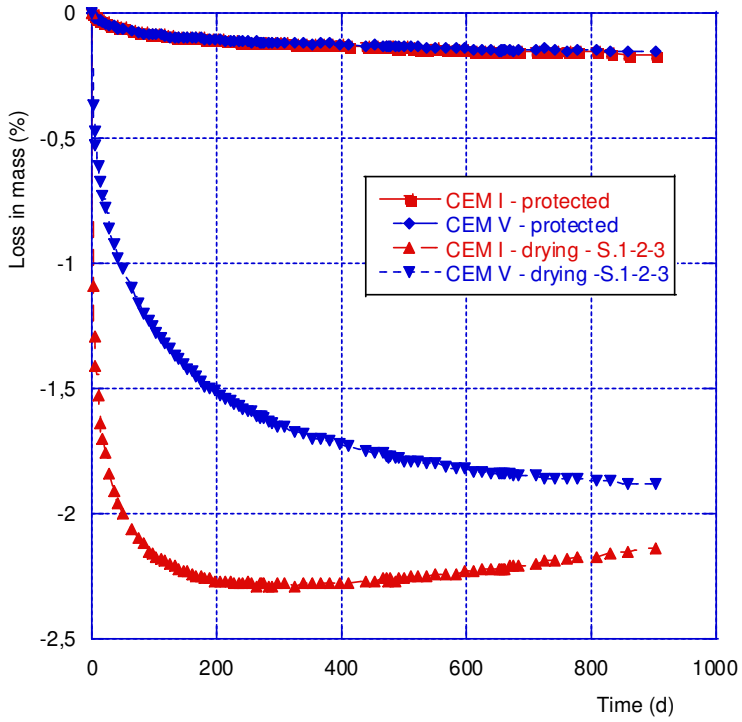

Figure 10: Comparison of relative mass variation between protected and under drying samples

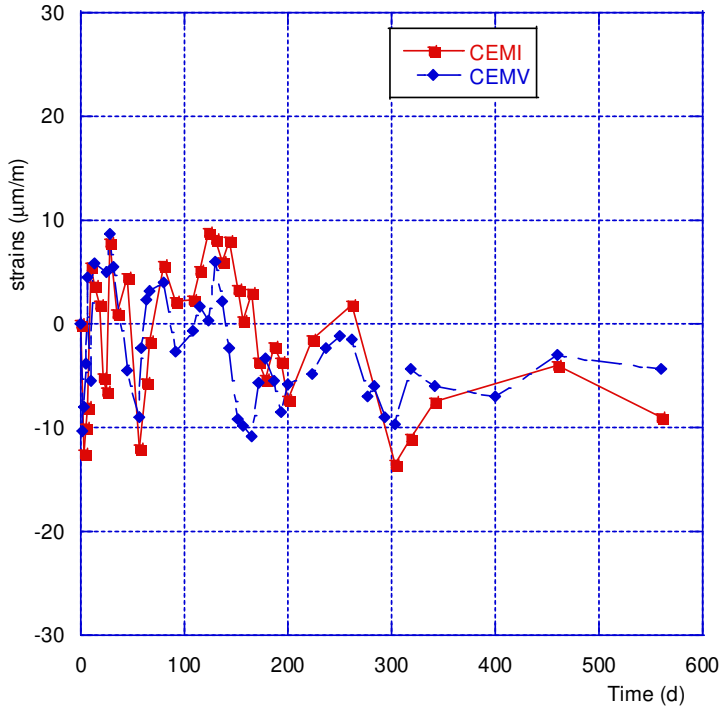

Figure 11: Strains recorded for non loaded-protected samples

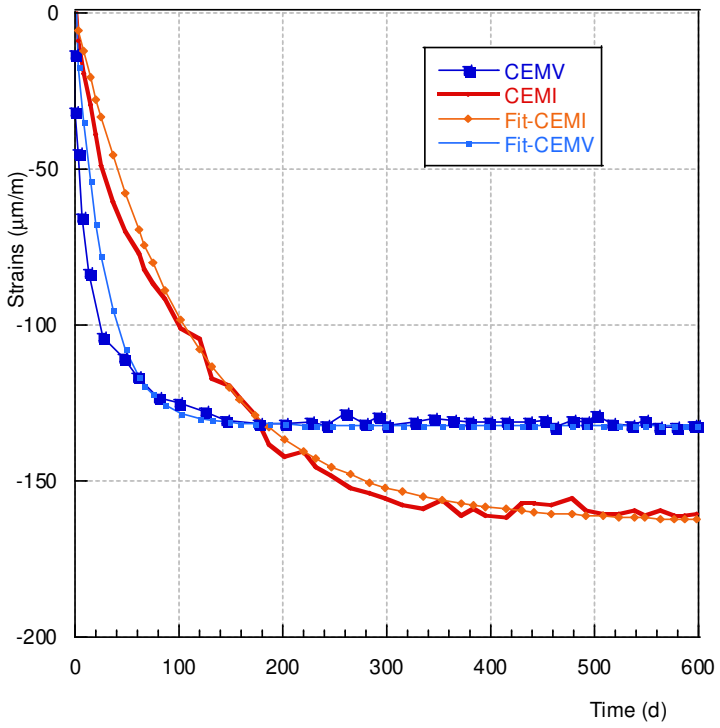

Figure 12: Strains due to basic creep for the two materials and fitting

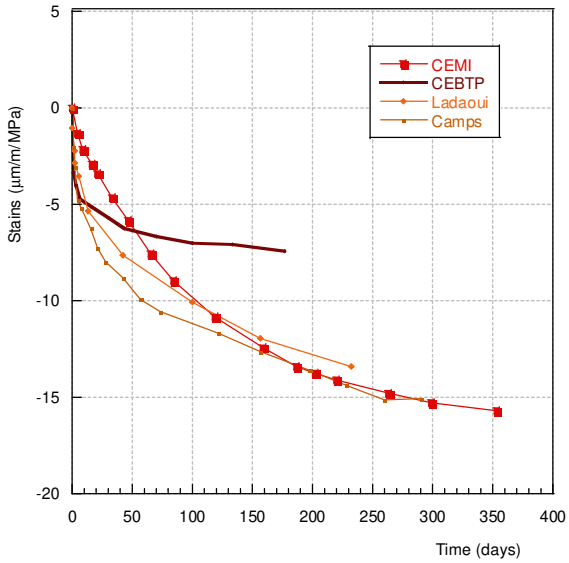

(a)

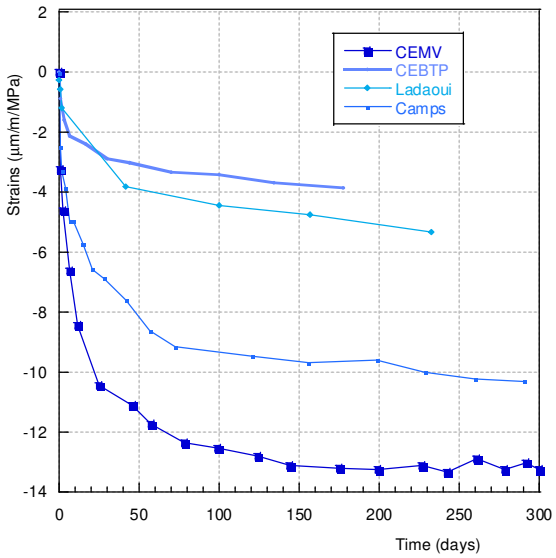

(b)

Figure 13: Comparisons between the present results (CEMI or CEMV) and those extracted from other studies

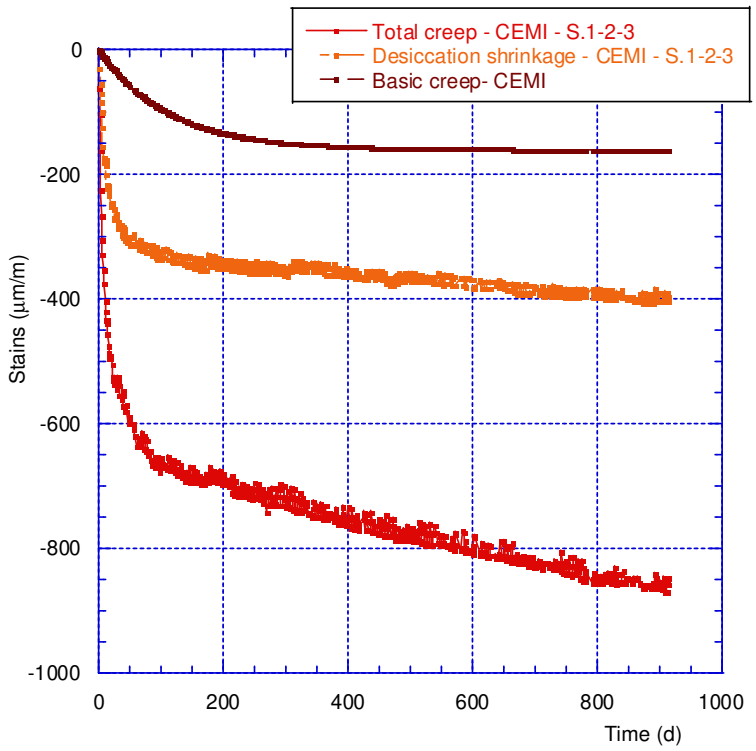

Figure 14 : Strains due to total creep, desiccation shrinkage and basic creep recorded for the CEMI

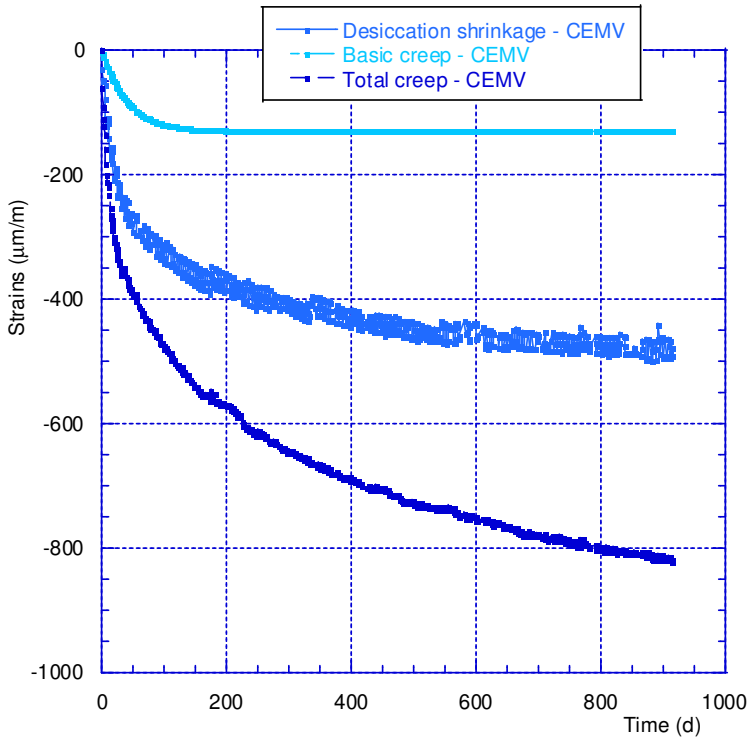

Figure 15 : Strains due to total creep, desiccation shrinkage and basic creep recorded for the CEMV

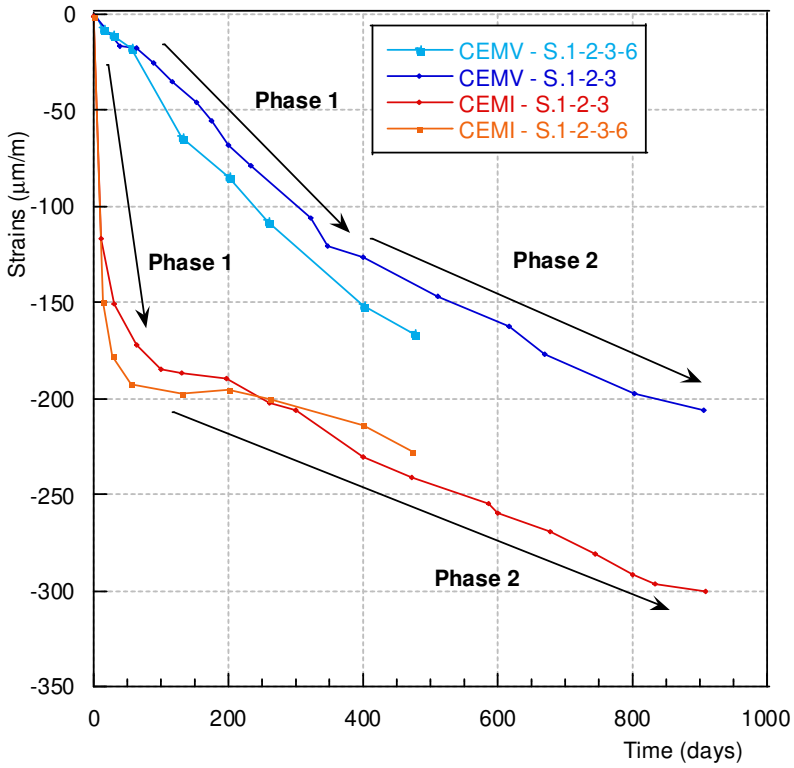

Figure 16: Strains due to drying creep for both concretes

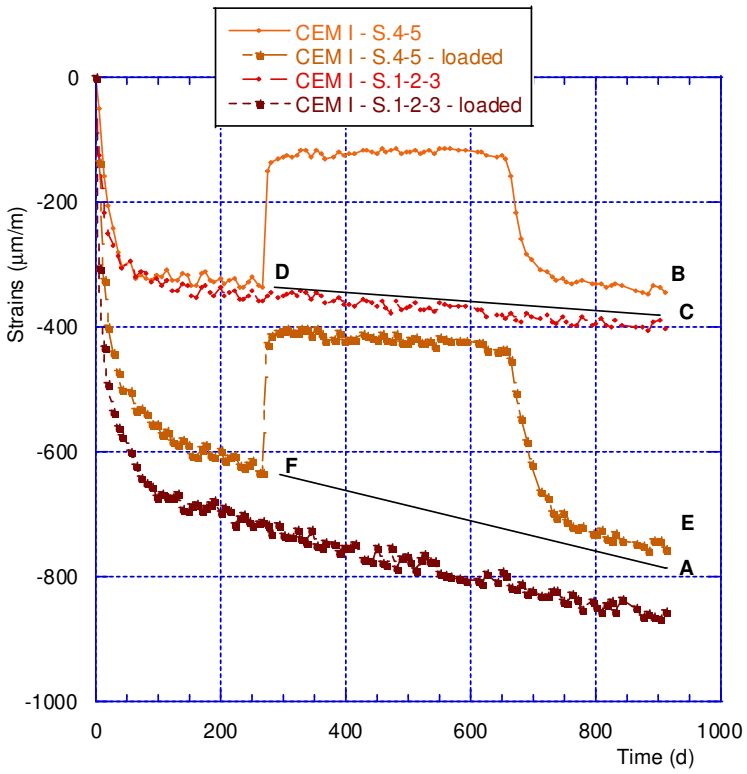

Figure 17: Strains vs time for the CEMI concrete – with the first cycle of drying-imbibition-drying

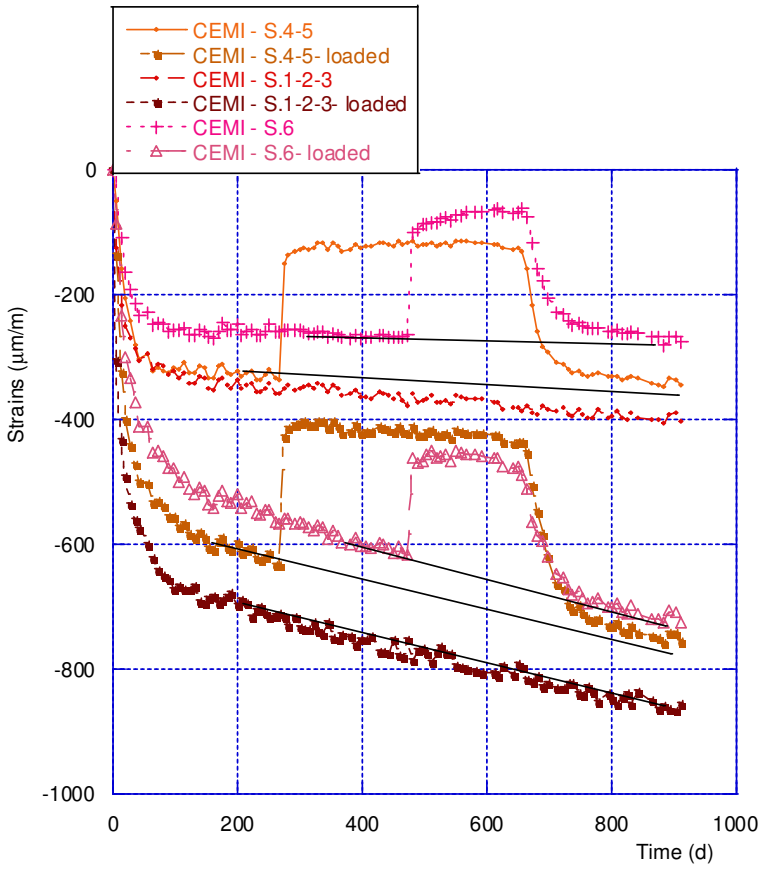

Figure 18: Strains vs time for the CEMI concrete – with the two cycles of drying-imbibition-drying

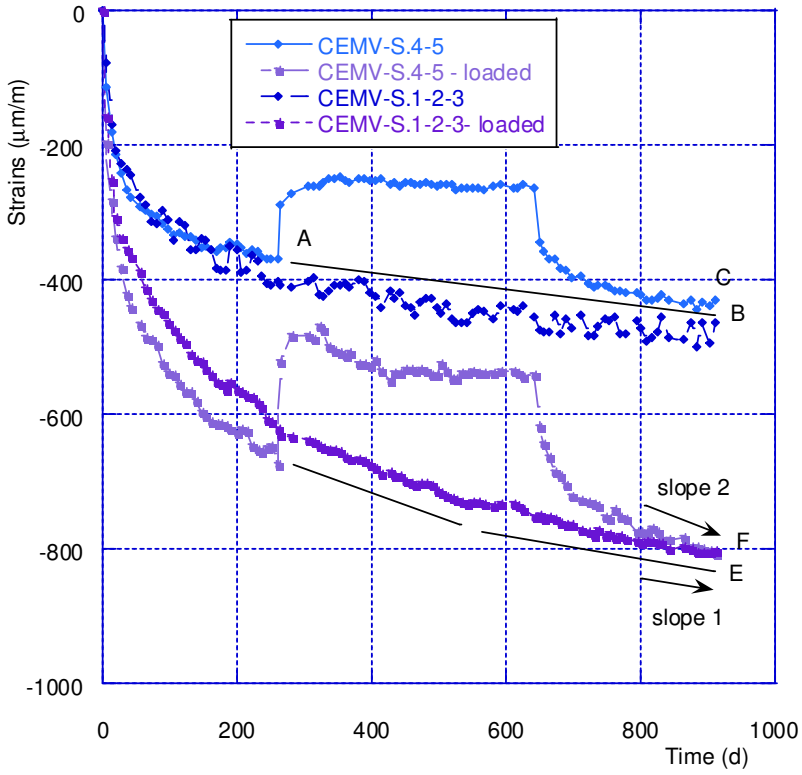

Figure 19: Strains vs time for the CEMV concrete – with the first cycle of drying-imbibition-drying

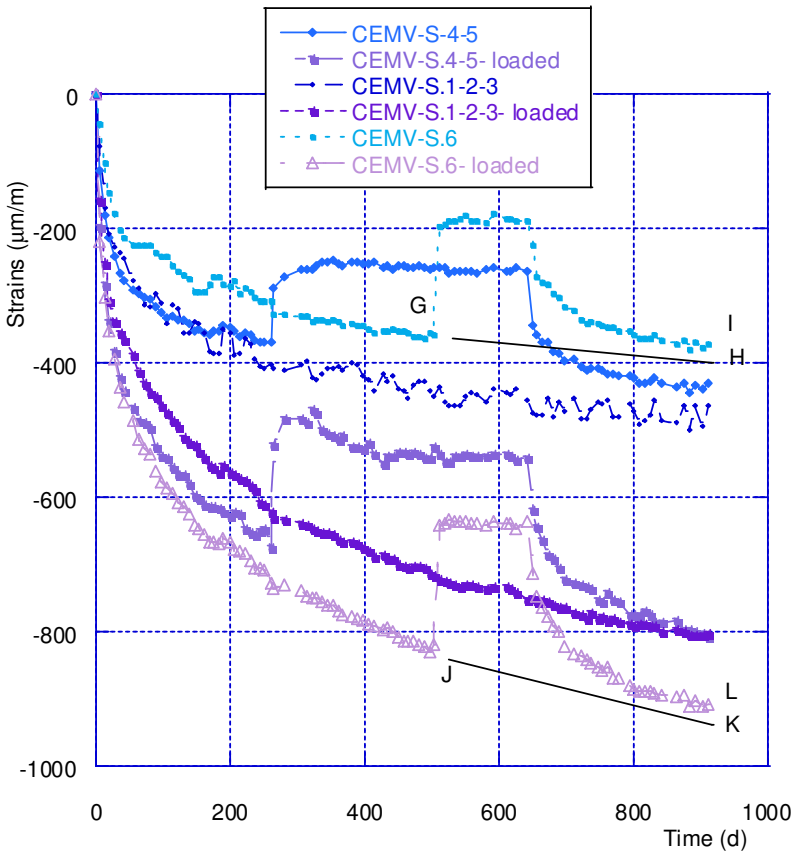

Figure 20: Strains vs time for the CEMV concrete – with the two cycles of drying-imbibition-drying

Tables

Table 1: Concrete formulations and properties. **Most values from [19] and [22].**

Concrete name	CEMI			CEMV		
Component	Nature	Source	Quantity (kg/m^3)	Nature	Source	Quantity (kg/m^3)
Cement	CEMI 52.5 R	France	400	CEMV/A 42.5 N	France	450
Sand	Limestone [0-4mm]	Boulonnais quarry, France	858	Limestone [0-4mm]	Boulonnais quarry, France	800
Gravel	Limestone [5-12mm]	Boulonnais quarry, France	945	Limestone [5-12mm]	Boulonnais quarry, France	984
Superplasticizer	Glenium 27	BASF	10	Glenium 27	BASF	11.5
Water (W/C)	-	-	171 (0.43)	-	-	173.3 (0.39)
Gas permeability (from literature)		$5.10^{-18}m^2$			$2.10^{-18}m^2$	
Porosity % (105°C)		**11,5%**			**12.8%**	
Compressive strength (MPa)		**73**			**69**	
Young Modulus (GPa)		**49**			**42**	

Table 2: Measurements performed and external conditions applied on samples

State	Mass measurements		Strain measurements Non-loaded		Strain measurements Loaded (10MPa)	
	CEM1	CEM5	CEM1	CEM5	CEM1	CEM5
Initial (Endogenous)	1	1	1	1	1	1
Drying (RH 50%)	3	3	3	3	3	3
Drying/Rewetting	(2+1)	(2+1)	(2+1)	(2+1)	(2+1)	(2+1)

Table 3: Generic numbering of samples

	Drying (RH50%)	Drying/Rewetting/Drying	Drying/Rewetting/Drying
Time (d)	900	260/654/900	460/654/900
Samples n°	1-2-3	4-5	6